Mixing and the Evolution of Cloud Droplet Size Spectra in a Vigorous Continental Cumulus

ILGA R. PALUCH AND CHARLES A. KNIGHT

National Center for Atmospheric Research,[1] Boulder, CO 80307

(Manuscript received 14 September 1983, in final form 19 March 1984)

ABSTRACT

Aircraft measurements in a vigorous, highly turbulent continental cumulus show predominantly bimodal and multiple peaked cloud droplet spectral shapes. The data are 100 m (1 s) averages. Three factors involved in the development of the cloud droplet size spectrum are discussed. First, evidence is given for local activation, far above cloud base, of significant concentration of new cloud droplets. This evidence is that strong peaks in the concentration of very small droplets are found in this data set and are in one-to-one correspondence with the simultaneous occurrence of a low concentration of the larger cloud droplets and a vigorous updraft. Second, a simple model of droplet sedimentation and evaporation at boundaries between clear, unsaturated air and cloud air, as occurs during entrainment, shows the development of broad and bimodal droplet spectra in boundary zones in periods of a few tens of seconds. Third, an analysis of the relation between the droplet size and concentration at the large-droplet peak of the spectrum shows nearly constant size at constant altitude regardless of major concentration variations. The only explanation of this fact that we have found is speculative and postulates the existence of major, small-scale nonuniformities in the droplet population. If true, this would in turn seem to imply that the turbulence is not fully developed to the smallest scales in the cloud studied.

1. Introduction

It has long been recognized that the rate of precipitation formation through the water phase is sensitive to the width of the cloud droplet size spectrum, and that diffusional growth calculations in an adiabatic parcel result in a narrower spectrum than is commonly observed except within a few hundred meters of cloud base. Broader cloud droplet spectra have been produced in microphysical models by including mixing of cloud with environmental air and recycling of air parcels within cloud, but the degree of broadening has been found to be quite sensitive to the mixing parameterizations employed and other model assumptions. At present, there is little agreement as to which sets of assumptions are the more realistic.

The primary question is, What happens to cloud droplets during mixing? While turbulent eddies disperse the entrained air, the ultimate homogenization of temperature and water vapor content takes place through molecular diffusion. Near the interfaces between cloud and entrained air, molecular diffusion produces undersaturation and cloud droplets tend to evaporate. If turbulent eddies stretch and entwine the entrained volumes so rapidly that the average time period a droplet spends near an interface is much less than the time it takes for the droplet to completely evaporate, then all droplets evaporate as if they had been exposed to the same average subsaturation. This extreme case is generally called *homogeneous mixing,* and it is implicit in numerical treatments of mixing commonly used in cloud modeling, where the water vapor contents and temperatures of cloud and entrained air are first averaged, and then all cloud droplets are allowed to evaporate until saturation is reached.

Laboratory studies by Latham and Reed (1977), however, did not support the homogeneous mixing hypothesis. More recently, Baker and Latham (1979) and Baker *et al.* (1980) have shown, using dimensional arguments, that the time scale for droplet evaporation in dry entrained air is typically much shorter than the time scale for turbulent mixing. They argued that the order of the two steps in the mixing calculations should be reversed: first, a fraction of the cloud droplets should be allowed to evaporate completely into the entrained volume until it is saturated and then the cloud and entrained air properties should be averaged. This parameterization decreases the concentration of cloud droplets without decreasing their size, in contrast to the homogeneous mixing parameterization in which all droplets decrease in size but none are lost in the mixing process, provided the air parcel does not become subsaturated. Because it produces lower droplet concentrations, it also produces higher supersaturations (or subsaturations) than homogeneous mixing, when air parcels ascend (or descend) following the mixing.

Baker and Latham's (1979) mixing model uses *in-*

[1] The National Center for Atmospheric Research is sponsored by the National Science Foundation.

homogeneous mixing and this phrase will be used in what follows only to refer to the local mixing process, not to indicate synonymity with Baker and Latham's entire cloud mixing model. We will define our usage of "homogeneous" and "inhomogeneous" more carefully in Section 5.

It is important to determine scales over which mixing may be regarded as homogeneous or inhomogeneous. If we view the cloud as consisting of many air parcels each mixed in different proportions, then a substantial fraction of the air parcels may become subsaturated and evaporate all drops in the mixing process. As pointed out by Telford *et al.* (1984), in this situation mixing could be homogeneous within each air parcel but appear nearly inhomogeneous on larger scales. The diffusive model of turbulent mixing by Baker and Latham (1982) illustrates this point. In this model, cloud properties are transferred into an entrained volume (scale about 100 m) according to a prescribed turbulent mixing rate, whereas on the subgrid scale (about 10 m), the mixing is implicitly treated as homogeneous. The droplet spectra from this model are not very different from the inhomogeneous mixing case, because large numbers of droplets completely evaporate before the entrained volume is saturated.

More recent studies by Broadwell and Breidenthal (1982) and Baker *et al.* (1984) have abandoned the concept of turbulent gradient diffusion, and emphasize the existence of coherent structures and the time-dependent nature of the mixing process. The entrained volumes are thought to be dispersed into smaller and smaller (or narrower and narrower) units, but still unmixed, until the final, intimate mixing takes place very rapidly and at a very small scale. While some droplets may completely evaporate during the early stages of mixing, estimates based on dimensional arguments for fully developed turbulence indicate that the final, small-scale homogenization of the mixed volumes should take place very rapidly and produce an overall decrease in droplet size (Baker *et al.*, 1984).

A number of people have attempted to incorporate some aspects of the three-dimensional, time-dependent nature of the mixing process in microphysical parcel models (Mason and Jonas, 1974; Telford and Chai, 1980, 1983; Baker and Latham, 1982; Manton and Warner, 1982; Jonas and Mason, 1982; Telford *et al.*, 1984). As it is not possible to discuss all these models here in detail, only a few of the more recent ones will be summarized briefly.

In the entity type entrainment mixing model of Telford and Chai (1980) and Telford *et al.* (1984), dry air is entrained at the cloud top where, during mixing, cloud droplets evaporate until the entrained volumes are just saturated. Then this air descends as a cold, saturated stream, maintaining saturation by evaporation of droplets from more mixing. Cloud droplet spectra are computed within air parcels that cycle up and down in the cloud while mixing with this saturated but nearly droplet-free, mixed air from the cloud top. Because the droplet concentration in the recycled parcels is diluted, the droplets grow and evaporate faster than in unmixed air parcels, some new droplets are activated and a broad droplet spectrum results. The authors showed that this type of air parcel recycling can produce a variety of droplet spectra. The shape of the droplet spectra and the maximum droplet sizes here depend on the assumed air parcel trajectories and mixing histories. The computed droplet spectra are broad, bimodal or multiple-peaked, and the maximum droplet radius is sometimes as much as twice as large as the maximum radius in an unmixed air parcel.

In the multithermal model of Mason and Jonas (1974), successive thermals rise and decay while entraining residues of earlier thermals. Broad droplet spectra are produced in this model through mixing with air containing partially evaporated droplets from earlier thermals. In a more recent study, a modified version of this model deals with dry parcels of air entrained through the cloud top (Jonas and Mason, 1982). The model employs the entraining spherical parcel parameterization: the mixing rate is proportional to the parcel diameter and the vertical acceleration of the parcel depends on its buoyancy and momentum exchange with the surroundings. The parcels are initially a few hundred meters in diameter and mixing within the parcels is assumed to be homogeneous. The droplet spectra computed in the descending and ascending parcels show considerable variability, depending on the vertical motion of the parcels and the air mixing histories. The droplet spectra are often bimodal in shape and the droplet sizes are significantly smaller in downdrafts than in updrafts but, as opposed to the entity type entrainment model, there are no large differences in the maximum droplet size in the mixed and unmixed updraft regions. This is because many new droplets are activated in the mixed regions, preventing rapid growth of the larger droplets. At present there is little agreement about the importance of droplet activation. In some microphysical models (Lee and Pruppacher, 1977; Baker and Latham, 1982; and the preceding reference), large numbers of new droplets are activated, whereas in others (Warner, 1973; Manton and Warner, 1982), activation of new cloud droplets is minimal.

In the following sections, aircraft data from a continental cumulus cloud are examined in an attempt to infer which physical processes played important roles in the evolution of cloud droplet spectra and to what extent the observations are consistent with some model assumptions and mixing parameterizations. Because the analysis is limited to one cloud only, the present results and conclusions should not be interpreted as a general evaluation of the various modeling assumptions.

2. General cloud characteristics

The data were collected during the Cooperative Convective Precipitation Experiment (CCOPE) in southeastern Montana in one of a number of towering cumuli that grew on 9 June 1981. The cloud was selected because the data looked good and complete, and because most of the droplet size spectra were bimodal; explaining bimodality has been one of the themes of research on cloud droplet spectra. The cloud was in an active stage of development. During the 16 min when cloud penetrations were made, its maximum radar reflectivity increased from less than 20 to 50 dBZ. The cloud was 4–5 km wide, 5–6.5 km high [from cloud base to the 0 dBZ radar top] and contained updrafts up to about 17 m s^{-1}. The cloud base was at 4°C, 790 mb, 2 km (MSL). Data from the nearest sounding and aircraft cloud base measurements from NCAR Queen-air 306D indicate that the cloud adiabatic temperature excess could be as high as 5°C. However, no adiabatic cloud regions were observed from the Wyoming King Air flying 2.3–3.6 km above cloud base. The cloud there was highly turbulent and the recorded turbulent eddy dissipation rates reached 10^3 cm^2 s^{-3}. Very strong environmental wind shear, about 4×10^{-3} s^{-1} through the 6.5 km cloud layer, undoubtedly contributed to the turbulence.

At the time of the cloud penetrations, the cloud top had already reached an altitude where the potential temperature of the environment was too warm to produce significant penetrative downdrafts. However, it is conceivable that entrainment from lower levels, through the cloud top when the cloud was smaller or through its sides at some later time, may have produced penetrative downdrafts and air parcel recycling similar to that modeled by Telford and Chai (1980) or Jonas and Mason (1982).

3. Droplet spectra

Figure 1 shows cloud droplet spectra measured with the Forward Scattering Spectrometer Probe (FSSP) on the Wyoming King Air (Cooper, 1978), averaged over 100 m (1 s) intervals. Spectrum (a) was obtained in the strongest updraft recorded and it has the highest droplet concentration, but neither the liquid water content nor the temperature there reached adiabatic values. Spectrum (b) was measured at a greater altitude than (a) in a weak downdraft near cloud edge. It is similar in shape to spectrum (a) but contains fewer droplets. Spectra (c) and (d) are two consecutive measurements in a relatively strong updraft. Both are distinctly bimodal. There are large differences in peak concentrations, but the two peaks occur at the same droplet sizes. In general, the radius at smaller peaks varies, as is illustrated by (d) and (e). On occasion there are several peaks at small droplet sizes, as in (f), and sometimes the spectrum is quite broad, as in (g) and (h), suggesting that it may contain a number of unresolved peaks.

Table 1 shows the frequencies with which the several spectral shapes were observed. As the penetration altitude increases, the relative frequency of spectra with only one peak decreases and the spectra become predominantly bimodal. While the data presented here are limited to the first cloud investigated on 9 June, other clouds penetrated nearby had rather similar droplet spectra. Spectra with two or more peaks are not uncommon (Warner, 1969; Skhirtladze, 1980), though on this flight, such spectra were observed with an unusually high frequency.

Recently, considerable effort has been expended in calibrating the FSSP probes (Cerni, 1982; Baumgardner and Dye, 1983). No attempts have been made to apply these corrections to the present FSSP data because the discussion is not sensitive to the exact droplet size and concentration.

4. Activation of new cloud droplets

In numerical models, bimodal droplet spectra often result from activation of new droplets when the supersaturation in an air parcel exceeds the peak supersaturation it had experienced near cloud base. If the observed bimodal and multimodal distributions were due to new droplet activation, then the concentration of small droplets should depend on the supersaturation the cloud air had experienced earlier. Seeking evidence of activation of new droplets within cloud, the data were examined for correlation between the presence of large concentrations of very small droplets and an estimate of a kind of conditional supersaturation, a supersaturation that would have been attained if the small cloud droplets were not present.

When the updraft velocity and the droplet size spectra are known, supersaturation can be computed using a steady state assumption that the condensation rate just balances the tendency for supersaturation to increase during ascent. For the data considered below, this equilibrium condition typically would be reached within a few seconds, less than 20 s even in the extreme cases of very low droplet concentration. The equations are given in the Appendix. The supersaturations are calculated using the measured vertical velocities. This procedure is valid to the extent that the updraft of the given parcel had not changed too much since the hypothetical droplet activation occurred; an assumption that is justified primarily by the nature of the correlation exhibited below.

The first two plots in Figs. 2, 3 and 4 show concentrations of droplets ≤ 6 μm in radius and supersaturations calculated as above, but in two ways: 1) using the droplets > 6 μm in radius only (solid lines—the conditional supersaturation) and 2) using all the droplets in the spectrum (dashed lines). As can be seen,

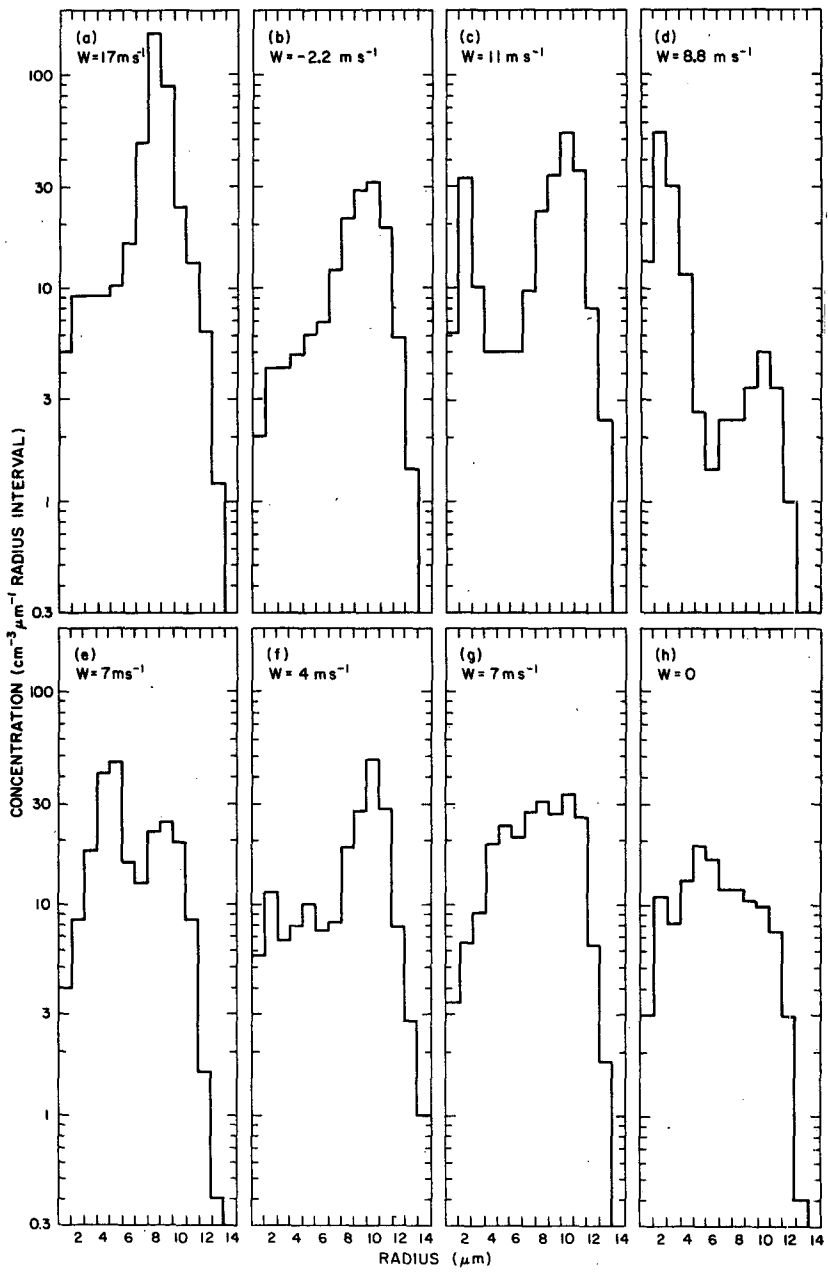

FIG. 1. Samples of cloud droplet spectra measured by FSSP over 100 m (1 s) flight paths. The vertical velocity (W) is indicated at the top of each panel. The positions in the updraft of samples a–d are marked in the vertical velocity plots in Figs. 2 and 3.

TABLE 1. The frequency with which different spectral shapes were encountered at different flight levels.

Penetration number	Approximate temperature (°C)	Frequency (%)		
		Single peak	Two peaks	Several peaks
1 and 2	−12	43	43	14
3 and 4	−15	19	69	12
5	−17	10	80	10
6	−2	0	81	19

there are cloud regions where the supersaturation would have been very high without the small droplets and these regions are associated with strong peaks in the concentration of small droplets. Except for the most prominent peaks in conditional supersaturation, all of which correspond to the highest peaks in concentration of small droplets, the rest of the data show little correlation between the two.

The vertical wind velocities have been calculated from the measurements of true airspeed, angle of at-

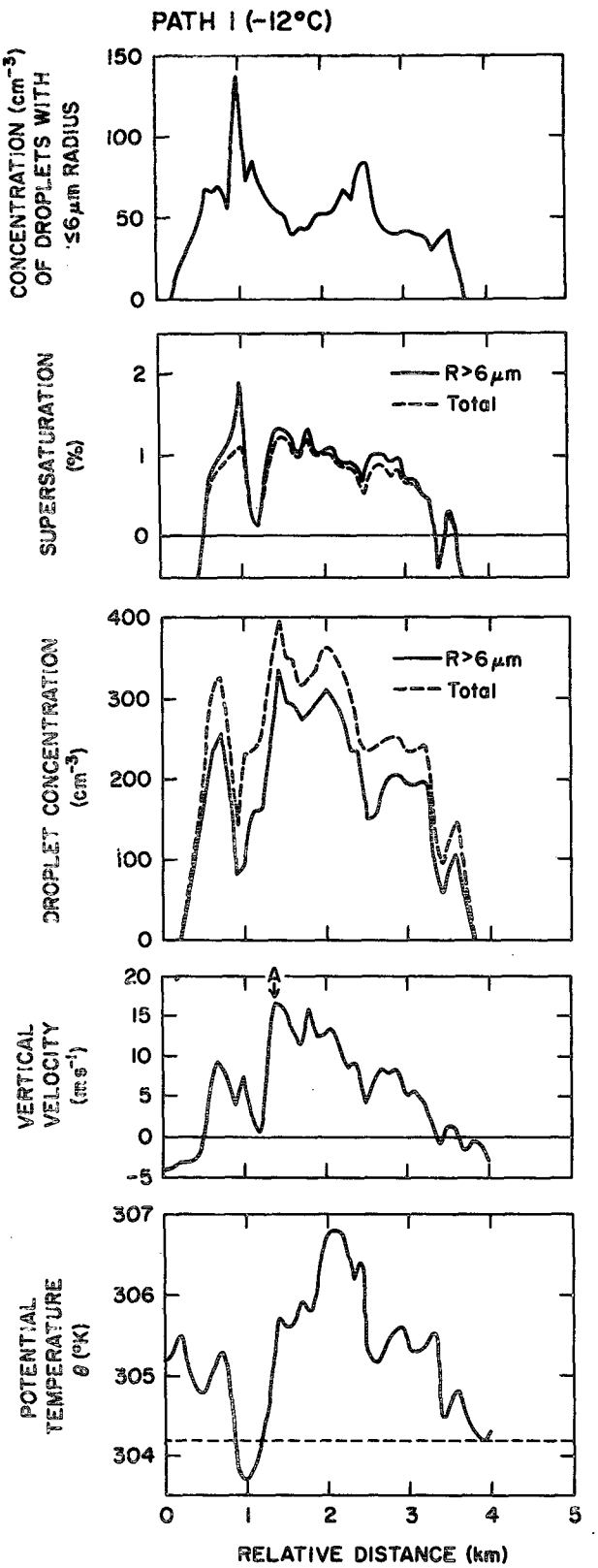

FIG. 2. Data collected during the first cloud penetration at about −12°C. For explanation see text.

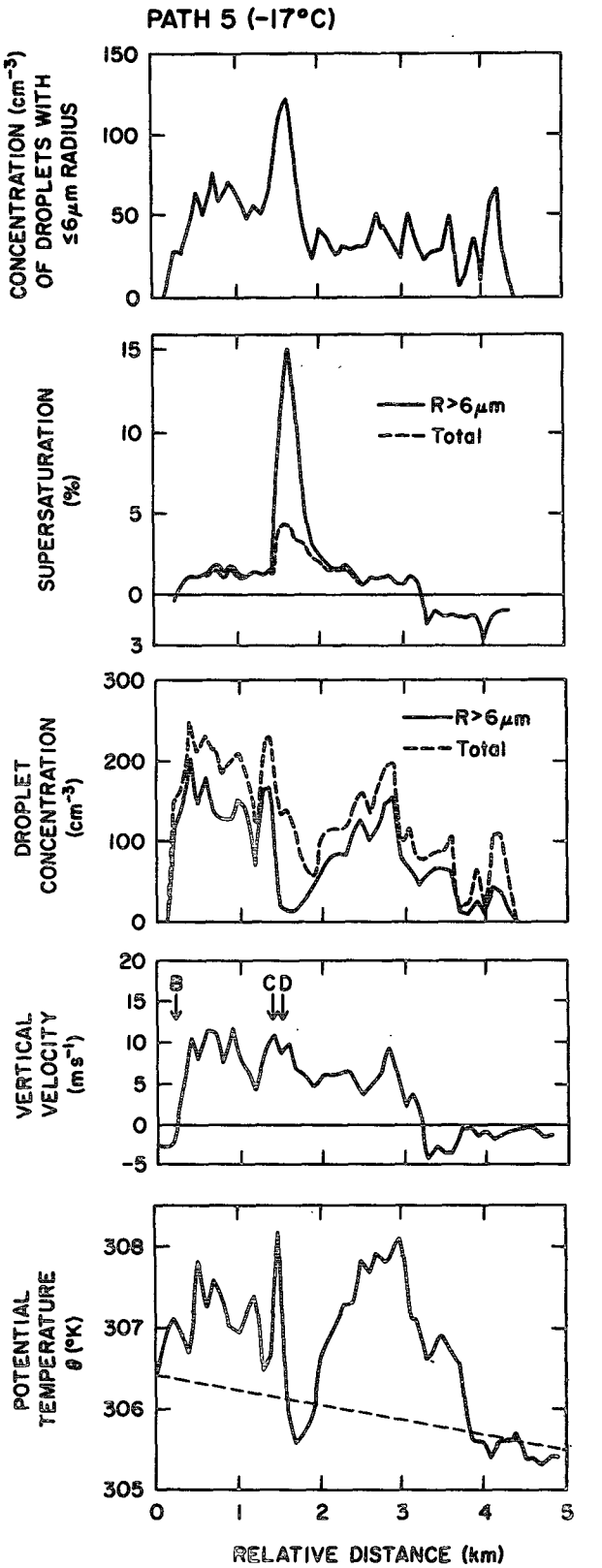

FIG. 3. As in Fig. 2 but during the fifth cloud penetration at about −17°C.

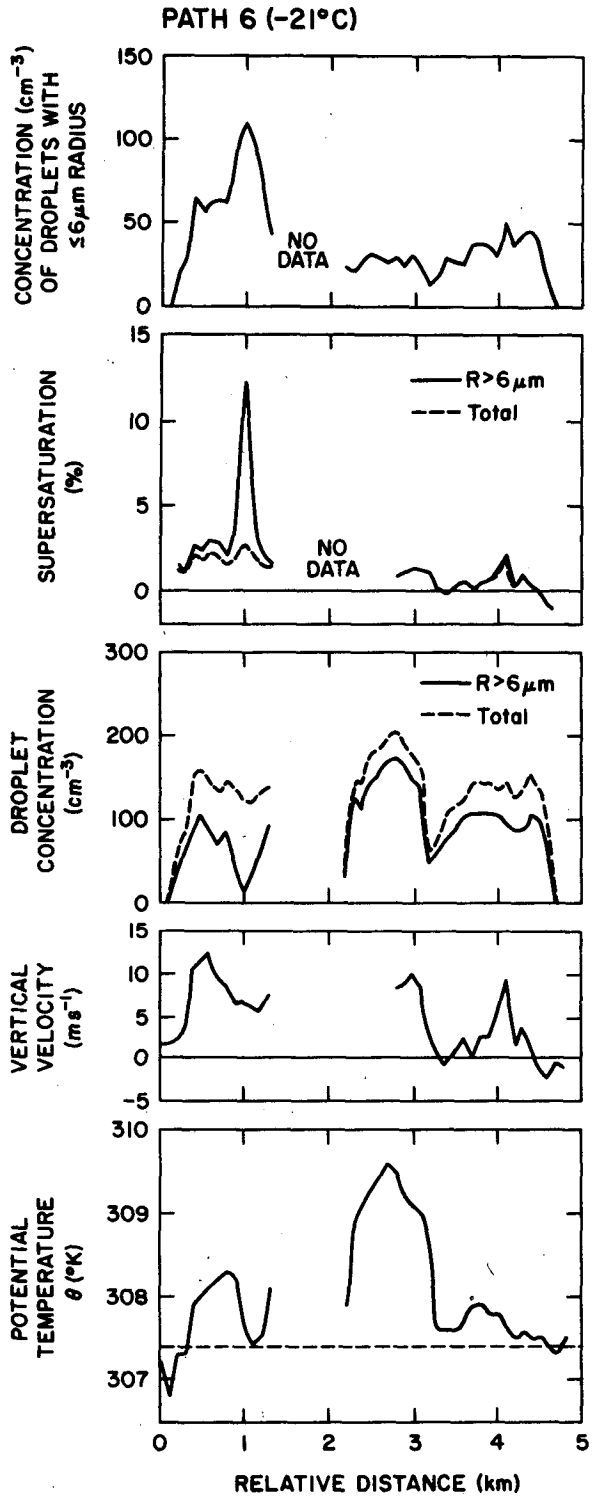

FIG. 4. As in Fig. 2 but during the sixth cloud penetration at about −21°C.

tack, pitch angle and vertical aircraft acceleration (Rodi, 1981). The vertical velocities are not reliable in and after turns, but the velocities associated with the peak supersaturations are thought to be sufficiently far away from turns not to be affected. In all cases, the vertical velocities at the peak supersaturations were relatively high (≥ 7 m s^{-1}) so that it is unlikely that these regions could have been in downdrafts. The peaks in the supersaturation arise primarily from low concentrations of large droplets rather than changes in vertical velocity. Moderate errors in vertical velocity (≤ 3 m s^{-1}) would change the magnitude of the computed supersaturations but not the position of the peak supersaturations.

It is difficult to account for the correlation of the prominent peaks in the computed supersaturation with those of small droplet concentration except by appealing to droplet activation. Let us assume that new droplets have been activated a short time prior to the measurements and that during this time the updraft has not changed. Then, the droplets would have experienced an average supersaturation that is less than the computed conditional supersaturation but more than the supersaturation computed using all of the droplets. If supersaturation is high, the growth times for small droplets are short: to reach 2 μm radius, this time is 36 s and 3.6 s at 1% and 10% supersaturation and, to reach 6 μm radius, 144 s and 14.4 s, respectively. In these estimates the length scale associated with the condensation coefficient is 5 μm. At high supersaturations the assumption that the updraft has not changed significantly since the droplets were activated does not seem unrealistic. Thus, we would expect some correlation between the computed conditional supersaturation and the concentration of small droplets when this supersaturation is high, but not when it is low, as indeed the data in Figs. 2–4 indicate. The correlation between the highest peaks in the conditional supersaturation and the highest peaks in the concentration of small droplets is therefore consistent with the activation of new droplets.

The third and fourth plots in Figs. 2, 3 and 4 show droplet concentrations and vertical velocities. The high conditional supersaturations are found in cloud regions where low concentrations of large droplets and relatively high vertical velocities coexist. The bottom plots in Figs. 2, 3 and 4 show cloud air potential temperature calculated from data from the reverse flow thermometer. This temperature fluctuates in phase with droplet concentration indicating that mixing rather than droplet depletion by growing precipitation is the main cause of low droplet concentrations. The dashed lines represent the potential temperature of the environment at the flight altitude, interpolated from data in the clear air at the ends of each penetration. As can be seen, even in highly mixed cloud regions the potential temperature is only a few tenths of a degree below that of the environment, whereas in the less mixed cloud regions the potential temperature excess is sometimes as high as 2 to 2.5 K. In clouds with less buoyancy,

mixing would be more likely to destroy the updraft entirely and thus the creation of high supersaturations, with concomitant activation of new droplets, would be less likely. This reasoning may indicate why this particular cloud has an exceptionally high incidence of bimodal spectra.

The observed higher incidence of bimodal spectra at higher altitudes is also consistent with new droplet activation, because as the altitude increases, the cloud air becomes more diluted through mixing, but the updraft remains relatively strong and thus more cloud volumes experience higher supersaturations (as can be seen by comparing Figs. 2 and 4).

Alternate interpretations of the observed spectra might be that the small droplets are due to evaporation from larger sizes, or that they are the result of mixing between different cloud volumes each having a distinctly different spectral mode. Either process would tend to produce a general, inverse correlation between the concentrations of large and small droplets. In Fig. 5, the concentration of droplets ≤ 6 μm in radius is plotted against the concentration of droplets > 6 μm in radius. The plot shows no such general correlation, implying that the above processes are not primarily responsible for the observed droplet spectra. The few points where the small droplet concentration is high when the large droplet concentration is low are associated with the prominent peaks in the computed supersaturation.

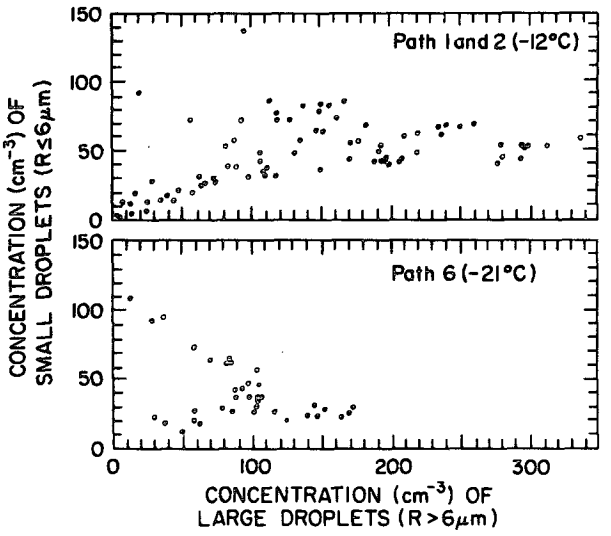

FIG. 5. Concentrations of small droplets (≤ 6 μm in radius) plotted against the concentration of large droplets (>6 μm in radius). The data are from the first two lowest and the last highest cloud penetrations. Similar distributions of points were obtained from the other penetrations.

5. Some details of the inhomogeneous mixing process

Mixing in real clouds takes place neither completely homogeneously nor completely inhomogeneously, but somewhere between the two extremes. Nevertheless, it is of some interest to compare the droplet spectra that the two extreme types of mixing would produce. Here and in the following discussion we consider the mixing of cloud with air well below saturation; the terms homogeneous and inhomogeneous mean that the time scale for turbulent mixing is, respectively, much smaller and much larger than that for droplet evaporation. While homogeneous mixing is expected to shift the droplet spectra toward smaller sizes, the consequences of inhomogeneous mixing are not straightforward when the effects of droplet sedimentation are taken into account.

Numerical simulations have been performed to study cloud droplet behavior near a boundary between cloud and unsaturated air. The calculations are one-dimensional and extend over short distances and time periods, during which turbulence is assumed to be absent and only molecular diffusion operates. Initially, the droplets have three discrete sizes: 8, 9 and 10 μm radius, containing 10^{-17}, 3×10^{-17} and 10^{-16} moles of dissolved NaCl and the droplet concentrations are 160, 80 and 40 cm^{-3} respectively. In the calculations the length scale associated with the condensation coefficient was set at 5 μm. The numerical simulations were performed using a revised version of a model described earlier (Paluch, 1971).

Figure 6 shows supersaturation and droplet radius as a function of distance, 30 s after cloud air has been in contact with air from the environment whose initial relative humidity is 40%. Sedimentation is neglected and this therefore represents a vertical cloud boundary. Initially, the cloud boundary is at 0 and as time progresses, it recedes to the right. After 30 s there is a 1 cm layer where all cloud droplets have evaporated and a 2 cm layer where the droplets have significantly decreased in size, but more than 2 cm away from the cloud boundary, the droplet sizes have not changed appreciably. The speed at which the cloud boundary recedes decreases with time because molecular diffusion slows down as the temperature and water vapor gradients decrease. If the initial relative humidity of the environment is increased to 80%, essentially the same thing happens but more slowly. In this case also, we find that droplets more than 2 cm away from the cloud boundary have not evaporated significantly.

Figure 7 represents the same situation as in the previous figure but with the droplets sedimenting into dry air: the cloud is above the entrained air and the boundary is horizontal. As before, the cloud boundary is initially at 0, but as the droplets fall, the cloud boundary moves into the entrained air, leftward in Fig. 7. After 30 s, a layer 14 cm thick has been saturated (Fig. 7a). The droplets in this layer consist of the initial cloud droplets which have not yet reached the descending

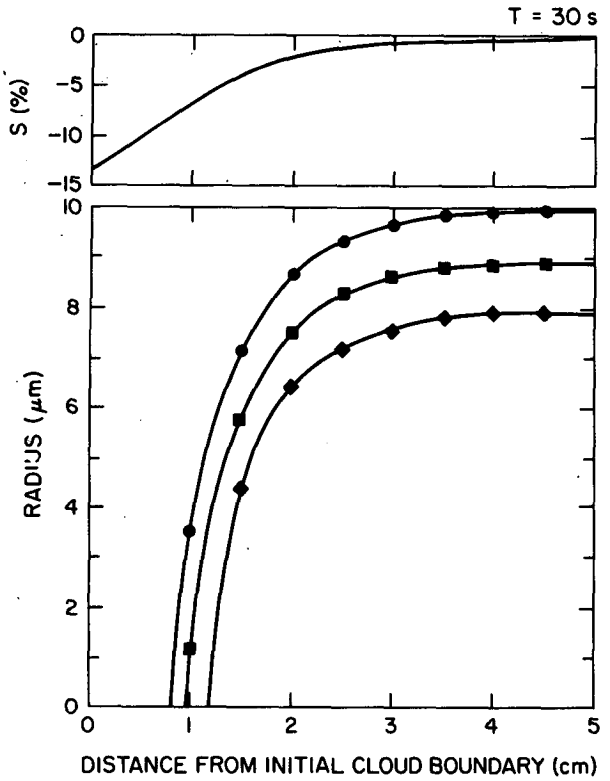

FIG. 6. Supersaturation and droplet radius as a function of distance from the initial cloud boundary 30 s after it has been in contact with air from the environment at 40% relative humidity. For initial conditions, see text. The calculations neglect droplet sedimentation (as when the cloud boundary is vertical) and turbulence.

interface, along with smaller droplets that have been at the interface and have partially evaporated there at some earlier time (Fig. 7b). These droplets do not completely evaporate because as their size decreases, their fall speed also decreases and they are overtaken by larger droplets which in turn evaporate and decrease the subsaturation. Droplets initially 10 μm in radius fall faster and penetrate deeper into the region of subsaturation where they completely evaporate, whereas the smaller droplets do not reach such high subsaturations and only partially evaporate. Fig. 7c shows an increase in droplet concentration near the cloud boundary, which comes about because of the decrease in fall speed there. Fig. 7d shows the overall droplet spectrum in the entrained volume, averaged from 0 to -16 cm. The large fluctuations in concentration at the smaller droplet sizes are due to the coarse subdivision of the initial spectrum. Had there been more subdivisions, the spectrum would have been smoother, more bimodal in shape. The initial cloud droplet spectrum (dashed lines) and the large droplet spectral peak in the entrained volume are quite similar, because the calculations assume that the overlaying cloud volume is sufficiently thick to allow new droplets to sediment continually into the entrained volume. Had this not been the case, the concentrations in the large droplet spectral peak would be lower, but the radius at the peak would remain unchanged. This peak only disappears after all droplets have come in contact with the interface.

Figure 8 represents the same situation as in Fig. 7, except that the initial relative humidity of the entrained air is 80%. Here the droplets undergo less evaporation. This is very similar to the result obtained by tripling the droplet concentration while keeping the relative humidity of the dry air at 40% as in Fig. 7.

Droplets also sediment at the lower boundary of a volume of clear air, leaving a region of cloud devoid of large droplets. In 30 s the 8 μm droplets will fall about 25 cm and the 10 μm droplets, 39 cm. In this way, droplet sedimentation can produce highly nonuniform droplet concentrations on a scale of 10 cm or more. Since molecular diffusion is very slow over such distances, this in turn can produce highly variable local supersaturations. A further consequence of this sedimentation process is that it tends to suppress the formation of the largest droplets, because they are the first to fall into subsaturated regions and evaporate.

As can be seen from Figs. 6, 7 and 8, droplet sedimentation from above saturates the entrained volume much more rapidly than does molecular diffusion. Thus, when cloud droplets are sufficiently large and mixing is inhomogeneous, the entrained volumes will become saturated primarily through droplet sedimentation, which will tend to produce a broad or bimodal droplet spectrum, nonuniform droplet concentration and preferentially evaporate the largest droplets.

6. How homogeneous is the mixing?

The processes of homogeneous and inhomogeneous mixing give rise to quite different, expected correlations between droplet size and concentration. In order to estimate expected magnitudes, calculations were performed for cloud conditions approximating cloud passes 3 and 4. The cloud air is at 560 mb, -15°C and contains 200 cm^{-3} droplets 10 μm in radius; the entrained air is at 33% relative humidity and -15°C. The solid lines in Figs. 9a and b show droplet concentration versus size for ideal homogeneous and inhomogeneous mixing, with position along the line corresponding to the amount of mixing. Results similar to the inhomogeneous case (Fig. 9b) are also obtained when the cloud air is mixed with premoistened entrained air (as in Telford and Chai, 1980). To see how sensitive the calculated values are to vertical displacement, the mixed air parcels were raised or lowered adiabatically about 300 m, giving a ± 0.3 gm kg^{-1} change in water vapor mixing ratio. This procedure is similar to the "intermittent mixing" assumed in some microphysical models (Telford and Chai, 1980;

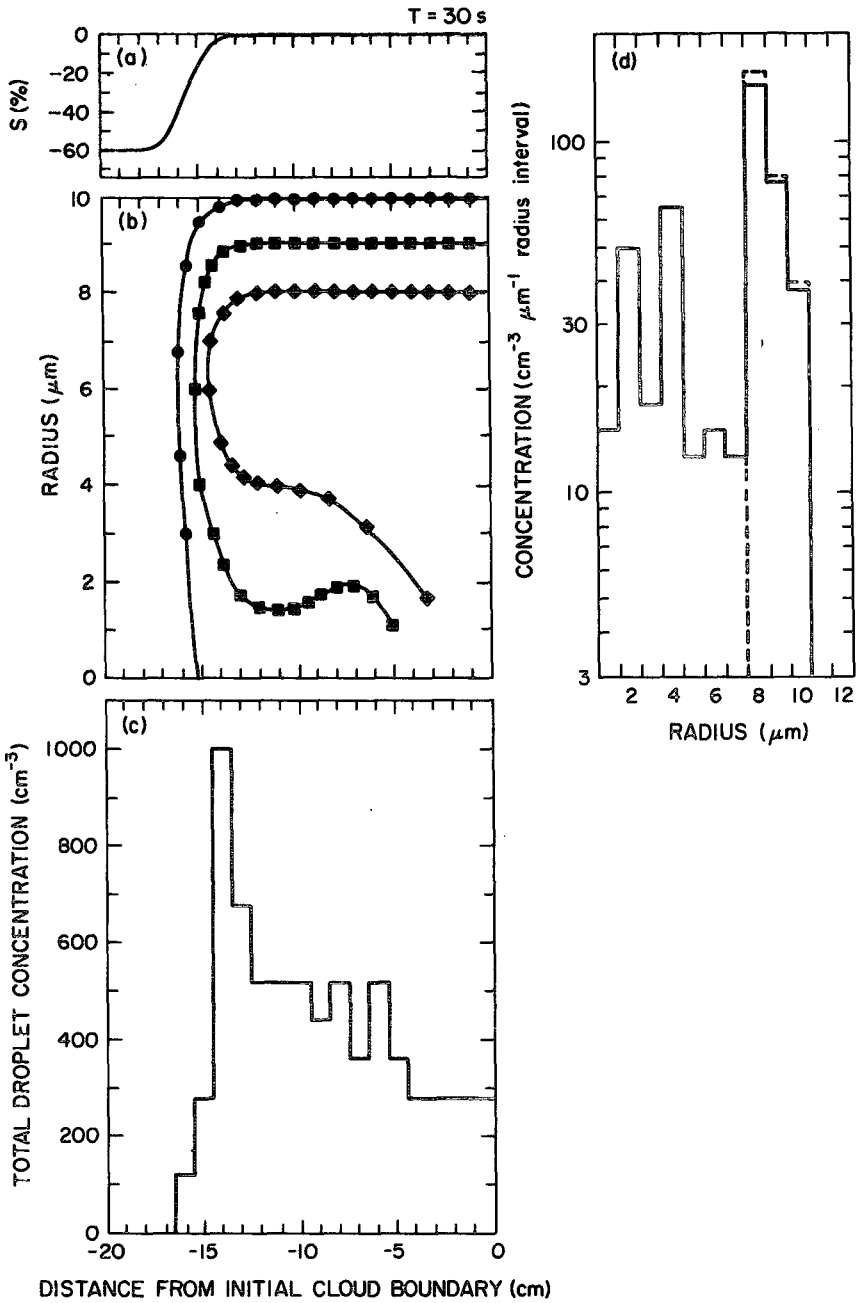

FIG. 7. (a) and (b) are as in Fig. 6 except that sedimentation is included (the cloud boundary is horizontal and the cloud is above the entrained air). Initially the boundary is at 0 and the droplets sediment to the left in the figure. (c) Total droplet concentration; (d) droplet spectrum in the entrained volume, averaged from 0 to −16 cm.

Baker *et al.*, 1980; Manton and Warner, 1982). The results from these calculations are represented by the dashed lines in 9a and b.

Earlier studies have used the mean droplet radius as an indicator of an overall change in the droplet spectrum. However, the mean radius is sensitive to the presence of small droplets which, as shown earlier, could have formed either by activation or by partial evaporation during inhomogeneous mixing. The mean radius is therefore not a reliable indicator of the overall shift of droplet spectrum toward a smaller size that is expected from homogeneous mixing. In the present data, most of the liquid water resides in the spectral peak at the large droplet sizes, whereas the small drop-

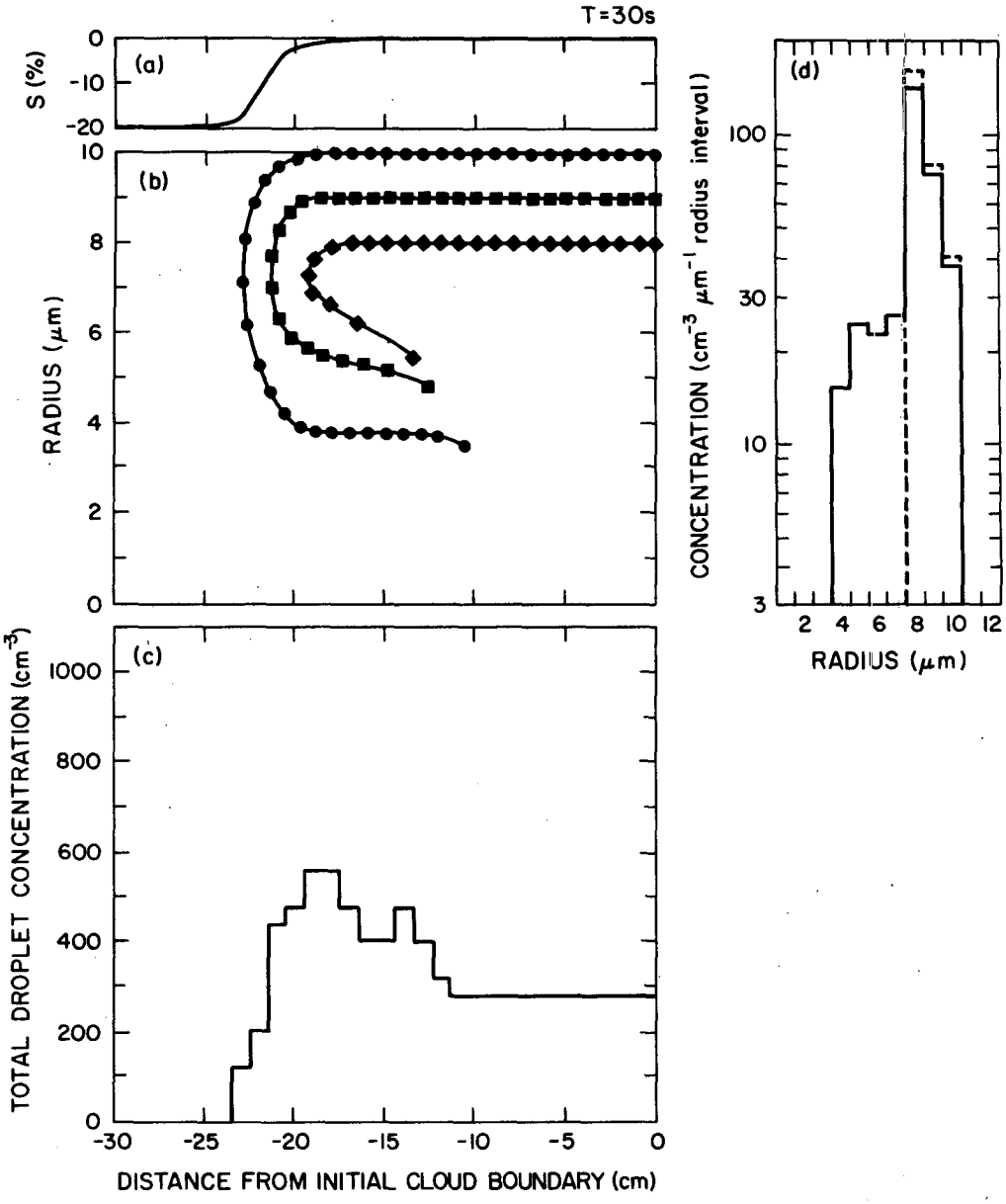

FIG. 8. As in Fig. 7 except the initial relative humidity of the entrained air is 80%.

lets (≤ 6 μm radius) contain less than 0.05 gm m^{-3} (~ 0.07 gm kg^{-1}) of liquid water. Usually the large droplet spectral peak is quite well defined and shows no large variations in shape (Fig. 1, a–f). In view of this, it was decided to use the radius at the large droplet spectral peak as the indicator of overall change in droplet size.

Figure 10 shows droplet concentration at the large droplet peak as a function of the radius at the peak. As in Fig. 1, the data are 100 m (1 s) averages. Cases where the peak is not resolved (as in Fig. 1h), which constitute 14% of the dataset, were excluded. (This was done by excluding spectra for which, at 3 μm above the radius at peak concentration, the concentration dropped by less than one-third of the peak concentration.) The shape of the spectrum at the large droplet end is relatively constant and when the large droplet peak is well resolved, the total droplet concentration in this peak is about 3 times the value at the peak itself, using the 1 μm radius interval. Since this peak is sometimes partially obscured by nearby peaks at smaller droplet sizes, the value of the peak itself has been used as an estimate of the total droplet concentration in the peak (left-hand scale in Fig. 10).

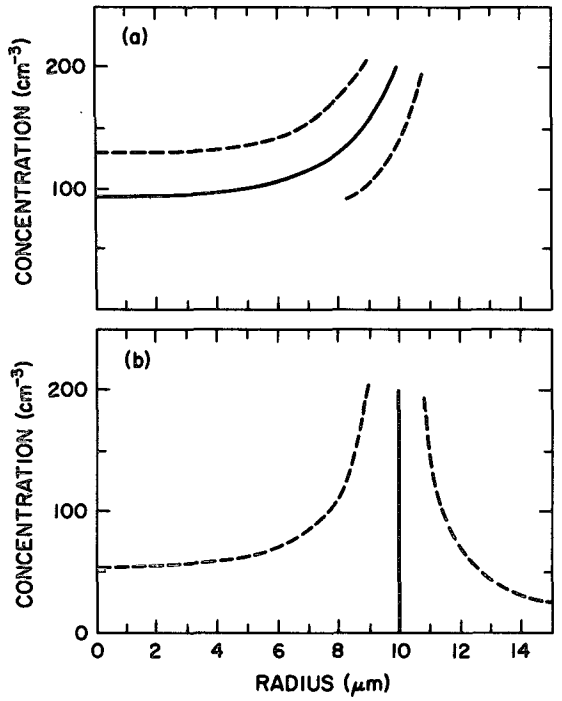

FIG. 9. Computed droplet concentration versus radius: (a) homogeneous mixing; (b) inhomogeneous mixing. Solid lines represent mixing at constant altitude at −15°C and dashed lines represent mixing followed by a change in altitude (about 300 m) that results in a 0.3 gm kg^{-1} change in the water vapor mixing ratio.

The droplet data in Fig. 10 show no systematic decrease of size with concentration.[2] Such a decrease would be expected if mixing were homogeneous over 100 m distances and involved unsaturated air. In particular, dilution of the large droplet peak down to a few tens per cubic centimeter without drastically reducing the size at the peak would be quite impossible in a homogeneous mixing process involving dry air (as for example in Fig. 9a). If mixing were for the most part homogeneous and the droplet samples contained some smaller scale, unmixed entrained volumes (as in Broadwell and Breidenthal, 1982, and Baker *et al.*, 1984), then we would still expect to see some variation in droplet size at the large droplet spectral peak because of the different mixing histories of different cloud volumes. However, in this situation the droplet size would not be as well correlated with the concentration as would be expected in ideal homogeneous mixing. The unvarying radius at the concentration peak of the larger droplets is more consistent with inhomogeneous mixing (as in Baker and Latham, 1979), or mixing with premoistened entrained air (as in entity type entrainment mixing in Telford and Chai, 1980), or precipitation scavenging, though (as noted in Section 4) the latter is probably not important here.

Regardless of the mixing model, the lack of variation in the radius at the large droplet spectral peak at low concentrations is surprising because relatively small changes in altitude following mixing should reproduce large changes in droplet radius when droplet concentrations are low (as for example in Fig. 9b). The data do not show this.

The growth or evaporation of smaller droplets has relatively little effect on the large droplet radius because, as noted above, the smaller droplets account for less than approximately 0.07 g kg^{-1} of liquid water, much less than what an altitude change of a few hundred meters would produce.

The lack of change in the radius at the large droplet spectral peak at low concentrations can be interpreted in two ways. First, the mixed cloud regions might tend to remain at the altitude where most of the mixing had taken place and the observed vertical motions in these regions might be due to turbulent eddies too shallow to produce altitude changes that result in marked changes in droplet radius. This is unlikely because the observed droplet concentration is sometimes so low that even very small changes in altitude should produce significant changes in droplet radius. Given the observed vigorous vertical velocities, it is difficult to believe that no such changes in altitude had occurred. Second, it is possible that the mixed air parcels may have undergone significant changes in altitude, but the droplet concentrations are nonuniform on scales not resolved in the data and the observed droplet spectra consist primarily of droplets from cloud volumes where the local concentrations are high. Assuming this second explanation, a rough idea of the dominant concentration can be obtained from the observed average changes in droplet radius with altitude. From the lowest to the highest penetration (4.4 to 5.6 km) the radius at the large droplet spectral peak increases from about 9 to 11 μm. Over this distance there is approximately 1.2 gm kg^{-1} of water vapor available for condensation and the observed changes in radius correspond to a concentration of about 330 cm^{-3} (460 cm^{-3} if the final radius is 10.5 μm and 250 cm^{-3} if it is 11.5 μm). Concentrations measured over 100 m distances were typically well below this value, which is consistent with this second possible explanation and implies the existence of small-scale regions with very low droplet concentrations inside the cloud.

In fact, it seems difficult to explain the very specific size at the large droplet peak without it being simply the size that adiabatic ascent from cloud base would

[2] Among the spectra that had no distinguishable peak at the large droplet sizes (and therefore are not included in Fig. 10), a definite shift toward smaller sizes was observed on five occasions, when the concentration of droplets was very low (4 to 22 cm^{-3}). In four other cases, some shift toward smaller sizes may have been present. These cases, however, are relatively rare and constitute 2% (or 3.5%) of the dataset. None of the spectra excluded from Fig. 10 showed a shift toward larger sizes.

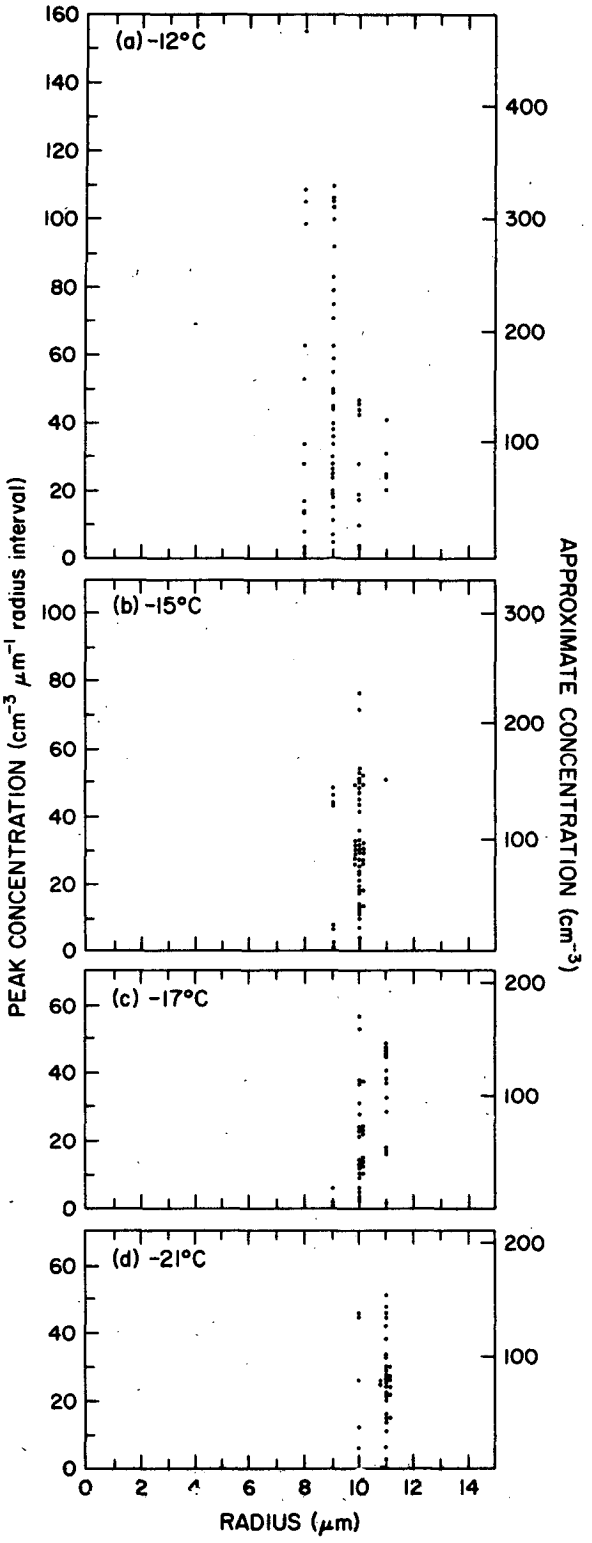

FIG. 10. Observed large droplet concentration versus radius at peak concentration: (a) and (b) contain two cloud penetrations each; (c) and (d) only one. Left-hand scale shows the concentration at the large droplet spectral peak; right-hand scale shows the estimated total concentration in this peak. The approximate penetration temperature is shown in the upper left-hand corner. The resolution of the FSSP corresponds to a 1 μm radius interval. In the plots, the data points are placed in the center of the radius interval, except when there is no room, in which case they are plotted nearby.

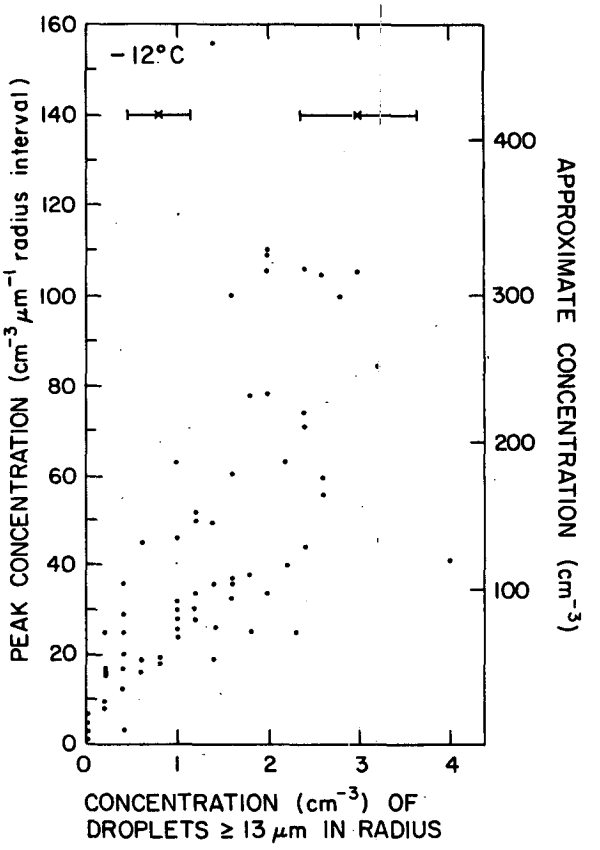

FIG. 11. Concentration of droplets equal to or larger than 13 μm plotted against the concentration at the large droplet spectral peak. The solid bars indicate the expected statistical errors.

produce. If it depends in some way on any mixing process, it should not be so constant and well-defined. In support of this, the large droplet spectral peak does not spread toward larger sizes at low droplet concentrations, as is sometimes the case in numerical models where mixed parcels produce some droplets that are significantly larger than those in unmixed parcels. In Fig. 11 the concentration of droplets ≥ 13 μm in radius is plotted against the concentration at the large droplet spectral peak. The data are from approximately the -12°C level and there were no droplets 15 μm or larger in concentrations above 0.1 cm^{-3}, the lowest detectable concentration for the FSSP. While the data show considerable scatter, there is some tendency for the concentration of droplets ≥ 13 μm to vary in phase with the concentration at the large droplet spectral peak, but certainly not the opposite. Data from other cloud passes show the same trend.

Finer scale measurements of cloud droplet spectra, averaged over 10 m distances, have been reported by Rodi (1981). These data show considerable variability in droplet concentrations between successive 10 m averages, but the radius at the large droplet spectral peak there too remains nearly constant regardless of droplet concentration. This suggests that there may be nonuniformities on scales less than 10 m. However, estimates assuming fully developed turbulence in the inertial subrange indicate that nonuniformities on such scales should be rapidly dissipated. For example, if the characteristic length scale of a cloud volume is 10 m and the turbulent eddy dissipation rate (ϵ) is 100 cm^2 s^{-3} then, on the basis of dimensional arguments (Tennekes and Lumley, 1972), this volume should be homogenized within 20 s ($\epsilon = L^2/T^3$ where L and T are the characteristic length and time scales respectively). It is, however, conceivable that we are dealing with turbulence that is not fully developed and that the cloud is not homogenized down to scales where molecular diffusion can operate effectively. The mixing process here could resemble the Broadwell and Breidenthal (1982) picture of mixing before the final stages of homogenization have been reached.

To summarize this section, the evidence from the large droplet peak presented in Fig. 10 seems to show that mixing remains incomplete at small scales. Other things being equal, one would have expected this cloud to be exceptionally well mixed because of its exceptionally high turbulence: thus, the evidence of incomplete mixing in this one cloud may apply to other less turbulent cumulus clouds. A great deal of this kind of data was taken in the two and one-half months of the CCOPE project, in clouds of different sizes, different stages of development and in different environments.[3] A qualitative inspection of data from other clouds on the same and several other days does reveal a few interesting exceptions, but for the most part supports the invariance of size with concentration at the large droplet spectral peak. However, it should be noted that most of these data were collected in the middle and lower cloud levels. It is possible that at the cloud top, mixing is more rapid and uniform. In the foregoing discussion we have not considered the origins of the entrained air and the extent to which the entrained volumes have been premoistened. While such information would be valuable, it can not be derived from the available data in this case.

7. Summary discussion

As presented above, the three discussions of factors involved in the development of the cloud droplet size spectrum have been quite separate. First, evidence was given for local activation, far above cloud base, of a significant concentration of new cloud droplets. This evidence is that strong peaks in the concentration of very small droplets are found in this data set and are in one-to-one correspondence with the simultaneous occurrence of a low concentration of the larger cloud droplets and a vigorous updraft. Second, a simple model of droplet sedimentation and evaporation at boundaries between clear, unsaturated air and cloudy air, as occur during entrainment, shows the development of broad and bimodal droplet spectra in boundary zones in periods of a few tens of seconds. Third, an analysis of the relation between the droplet size and concentration at the large-droplet peak of the spectrum shows nearly constant sizes at constant altitudes regardless of major concentration variations. The only explanation that we have found for this is speculative and postulates the existence of major, small-scale nonuniformities in the droplet population. If true, this would in turn seem to imply that the turbulence is not fully developed to the smallest scales in the cloud studied.

No strong claim has been made that the sedimentation–evaporation mechanism actually applies to the study cloud, particularly in view of its vigorous turbulence. However, if turbulence is not developed down to the scale at which molecular diffusion can homogenize the water vapor density in a few tens of seconds—a scale of the order of one centimeter—then the sedimentation–evaporation mechanism could indeed be important in the evolution of the droplet spectrum in this cloud.

It is interesting to us that the first and third conclusions seem somewhat contradictory, at least at first thought. The first conclusion implies that in some regions a considerable proportion of the air within the cloud is sufficiently mixed to be saturated, yet is quite deficient in droplets. These regions, furthermore, are rising fast enough for about 100 cm^{-3} of new droplets to activate. The third conclusion says that the mixing is generally not that intimate, because if it were, one should encounter some unusually large droplets at the lower concentrations, especially in the more modest updrafts, and this is not seen. One very speculative, possible reconciliation appeals to the sedimentation process itself. The largest droplets sediment fastest and so are least likely to spend very much time in the rather special environments conducive to exceptionally rapid growth, which may occupy relatively small cloud volumes. It is probably not fruitful to pursue such speculation very far, however, especially since the third "conclusion" can be tested directly.

Acknowledgments. We are grateful to the University of Wyoming Cloud Physics group for providing their aircraft data. We thank Joanne Parrish and Robin Vaughan for help in data processing, Dr. James Dye

[3] The CCOPE data are, of course, available to anyone who wishes to pursue this or other kinds of analysis (Knight, 1982).

for valuable comments and Frances Huth for typing the manuscript. We also wish to thank the reviewers for constructive comments and criticisms.

APPENDIX

Supersaturation

The expression for supersaturation has been computed following the approach of Squires (1952) but using a somewhat different notation. In a parcel of cloudy air ascending with velocity W, the rate of change of supersaturation S is

$$\frac{dS}{dt} = c_1 W - c_2 \frac{dq_L}{dt},$$

where q_L is the liquid water mixing ratio and c_1 and c_2 are slowly varying quantities:

$$c_1 = \frac{Lg}{R_v T^2 c_p} - \frac{g}{R_a T},$$

$$c_2 = \frac{P}{\epsilon e_s} + \frac{L^2}{R_v T^2 c_p},$$

L the latent heat of condensation,
g gravitation acceleration,
T temperature (K),
c_p specific heat of air at constant pressure,
R_v and R_a specific gas constant for water vapor and dry air respectively,
P pressure,
ϵ ratio of molecular weights of water and dry air (0.622),
e_s saturation vapor pressure.

The above expression is derived in Pruppacher and Klett (1978) and other textbooks.

The droplets considered are sufficiently large to neglect surface tension and solute effects so that the rate of condensation is

$$\frac{dq_L}{dt} = \frac{1}{\rho_a} \sum^{i} n_i \frac{dm_i}{dt} = \frac{4\pi c_3 S}{\rho_a} \sum^{i} n_i r_i,$$

where

ρ_a the density of air,
n_i number of droplets per unit volume with mass m_i and radius r_i,

$$c_3 \approx \left[\frac{R_v T}{e_s D} + \frac{JL^2}{KT^2 R_v}\right]^{-1},$$

D diffusion coefficient for water vapor,
K thermal conductivity,
J mechanical equivalent of heat.

Substituting the above in the first equation, we get

$$\frac{dS}{dt} + c_4 S = c_1 W,$$

where

$$c_4 = \frac{c_2 c_3 4\pi}{\rho_a} \sum^{i} n_i r_i.$$

The solution for supersaturation gives

$$S = S_0 \exp(-c_4 t) + \frac{c_1}{c_4} W[1 - \exp(-c_4 t)],$$

where at $t = 0$, $S = S_0$ and at $c_4 t \gg 1$, $S = Wc_1/c_4$. The above derivation and the calculated supersaturation in Figs. 3–5 neglect the condensation coefficient. Had it been included, the summation in c_4 would include a factor of $(1 + a/r_i)^{-1}$ where a is the length scale associated with the condensation coefficient and the calculated supersaturations would be higher.

REFERENCES

Baker, M. B., and J. Latham, 1979: The evolution of droplet spectra and the rate of production of embryonic raindrops in small cumulus clouds. *J. Atmos. Sci.*, **36**, 1612–1615.

——, and ——, 1982: A diffusive model of the turbulent mixing of dry and cloudy air. *Quart. J. Roy. Meteor. Soc.*, **108**, 871–898.

——, R. G. Corbin and J. Latham, 1980: The influence of entrainment on the evolution of cloud droplet spectra: I. A model of inhomogeneous mixing. *Quart. J. Roy. Meteor. Soc.*, **106**, 581–598.

——, R. E. Breidenthal, T. W. Choularton and J. Latham, 1984: The effects of turbulent mixing in clouds. *J. Atmos. Sci.*, **40**, 299–304.

Baumgardner, D. G., and J. E. Dye, 1983: The 1982 cloud particle measurement symposium. *Bull. Amer. Meteor. Soc.*, **64**, 366–370.

Broadwell, J. E., and R. E. Rosenthal, 1982: A simple model of mixing and chemical reaction in a turbulent shear layer. *J. Fluid Mech.*, **125**, 397–410.

Cerni, T. A., 1982: Determination of the size and concentration of cloud drops with an FSSP. Rep. No. AS 138, Dept. of Atmos. Sci., University of Wyoming.

Cooper, W. A., 1978: Cloud physics investigations by the University of Wyoming in Hiplex 1977. Rep. No. AS119, Dept. Atmos. Sci., College of Engineering, University of Wyoming, 321 pp.

Jonas, P. R., and B. J. Mason, 1982: Entrainment and droplet spectrum in cumulus clouds. *Quart. J. Roy. Meteor. Soc.*, **108**, 857–869.

Knight, C. A., 1982: The cooperative convective precipitation experiment (CCOPE), 18 May–7 August 1981. *Bull. Amer. Meteor. Soc.*, **63**, 386–398.

Latham, J., and R. L. Reed, 1977: Laboratory studies of the effects of mixing on the evolution of cloud droplet spectra. *Quart. J. Roy. Meteor. Soc.*, **103**, 297–306.

Lee, I. Y., and H. R. Pruppacher, 1977: A comparative study on the growth of cloud drops by condensation using an air parcel model with and without entrainment. *Pure Appl. Geophys.*, **115**, 523–545.

Manton, M. J., and J. Warner, 1982: On the droplet distribution near cloud base of cumulus clouds. *Quart. J. Roy. Meteor. Soc.*, **108**, 917–928.

Mason, B. J., and P. R. Jonas, 1974: The evolution of droplet spectra

and large droplets by condensation in cumulus clouds. *Quart. J. Roy. Meteor. Soc.*, **100**, 23–28.

Paluch, I. R., 1971: A model for cloud droplet growth by condensation in an inhomogeneous medium. *J. Atmos. Sci.*, **28**, 629–639.

Pruppacher, H. R., and J. D. Klett, 1978: *Microphysics of Clouds and Precipitation.* D. Reidel, 714 pp.

Rodi, A. R., 1981: Study of the fine-scale structure of cumulus clouds. Ph.D. dissertation, University of Wyoming, 328 pp.

Skhirtladze, G. I., 1980: Result of a measurement of droplet size spectra in cumulus clouds. *Atmos. Oceanic Phys.*, **16**, 40–45.

Squires, P., 1952: The growth of cloud drops by condensation. *Aust. J. Sci. Res.*, **5**, 66–86.

Telford, J. W., and S. K. Chai, 1980: A new aspect of condensation theory. *Pure Appl. Geophys.*, **113**, 1067–1084.

——, and ——, 1983: Comment on "Entrainment and the droplet spectrum in cumulus clouds" by P. R. Jonas and B. J. Mason. *Quart. J. Roy. Meteor. Soc.*, **108**, 857–869.

——, T. S. Keck and S. K. Chai, 1984: Entrainment at cloud tops and droplet spectra. Submitted to *J. Atmos. Sci.*

Tennekes, H., and J. L. Lumley, 1972: *A First Course in Turbulence.* The MIT Press, 300 pp.

Warner, J., 1969: The microstructure of cumulus cloud. Part I. General features of the droplet spectrum. *J. Atmos. Sci.*, **26**, 1049–1059.

——, 1973: The microstructure of cumulus cloud. Part IV. The effect on droplet spectrum of mixing between cloud and environment. *J. Atmos. Sci.*, **30**, 256–261.